A Micromechanical Model for the Optimization of a Class of Viscoelastic Short Fiber-Composites

Y. M. Haddad and J. Feng*

Dept. of Mechanical Engineering
University of Ottawa
Ottawa, Canada K1N 6N5

* *Currently with Bombardier Transportation*

ABSTRACT

The effects of selected microstructural parameters, e.g., fiber-aspect-ratio, fiber off-axis angle and fiber volume fraction, on the damping and stiffness of polymeric fiber-composite systems are first examined. Quasi-static models are, then, developed by using a "*Forced Balance Approach*" to determine the mechanical response properties of a class of polymeric short fiber-reinforced composites, whereby the material is assumed to behave in a linear viscoelastic manner. Subsequently, simultaneous optimization of damping, stiffness and specific weight is carried out by using the so-called "*Inverted Utility Function Method*". The obtained results show that polymeric composites reinforced with short aligned-fibers have superior design flexibility as compared with those reinforced with long aligned-fibers.

1. INTRODUCTION

It is well known that lightweight fibre reinforced polymeric composites have higher specific strength and stiffness when compared with conventional materials, such as metals. Much effort has been devoted to the improvement and optimisation of these properties in various composite structures. Good vibration damping properties are also particularly important for composite structures used under dynamic loading, such as in aerospace structures, rotor blades, circuit boards, high-speed printer components, etc. Due in part to the extensive use of conventional structural materials, which in general have poor internal damping characteristics, the potential for significant improvement and optimisation of damping in advanced fibre reinforced composites has not been yet fully realized. Meanwhile, the realization of short fibre reinforcement

in composite structures is still quite limited. This may be primarily due to a much wider involvement, from scientists and engineers, with the development and use of long aligned (continuous) fibre composites.

In the conventional damping theory, the damping factor is often assumed to vary comparatively little with frequency for a large class of polymers, at temperatures near their glass-transition temperature (Nashif *et al.* /1/). Consequently, a large number of researchers considered the damping factor for this class of materials to be constant. However, in the case of fiber-reinforced polymeric composites, and in particular short-fiber composites, the damping factor is not only a frequency dependant, but it also varies considerably with the micro-structural characteristics, e.g., fiber-aspect-ratio, fiber volume fraction and fiber off-axis angle, e.g. Gibson and Yau /2/, Gibson *et al.* /3/, Sun *et al.* /4/ and Suarez *et al.* /5/.

The damping properties of long aligned-fiber polymeric composites have been studied by a number of researchers, e.g., Bert and Clary /6/ and Bert /7/. There are, however, relatively few reports concerning the damping of short-fiber composites. In this context, studies reported, for instance, by McLean and Read /8/ and Gibson *et al.* /3/, indicate that vibration damping properties of fiber-reinforced composites with polymeric matrix may be significantly improved and may be readily optimized by using, as a reinforcement, short rather than long (continuous) fibers.

A possible explanation for the above-mentioned advantages concerning the damping of short-fiber composites is the presence of shear stress concentration at the ends of fiber-segments, and, thus, the resulting shear loading transfer mechanism between the reinforcement and the matrix material. The research work of Gibson and Yau /2/ and Gibson *et al.* /3/ indicates that by varying the fiber-aspect-ratio and fiber orientation, superior damping and stiffness properties could be achieved separately. This observation implies that the optimum conditions, in terms of microstructural parameters, for damping may not be necessarily the same for stiffness. Consequently, it is important to study the influence of the various governing microstructural variables as pertaining to both damping and stiffness. The optimization, in terms of the microstructure, of this trade-off between damping and stiffness is the main intention of this paper.

It is obvious that the most ideal situation for designing a short fiber-reinforced polymeric composite is to optimize the damping and stiffness simultaneously with respect to the microstructure controlling parameters. In this context, the general procedure of the "*Force-Balance Approach*", e.g., Sun *et al.* /4/, is used in this paper to formulate an analytical model pertaining to the optimization of the damping and stiffness of a class of short fiber-reinforced composites. Here, a multi-objective optimization functional is established to optimize these two properties simultaneously.

2. INFLUENCE OF SELECTED MICROSTRUCTURAL PARAMETERS

There appear to be two primary sources of enhanced damping in a polymeric matrix composite:

(i) the viscoelastic nature of the bulk matrix, and

(ii) the friction mechanism at the fiber/matrix interface as caused by the relative motion between the matrix and the fiber.

Both of these effects may prove to be significant in the case of short-fiber composites whereas high shear stresses are developed at the fiber-matrix interface. When a short-fiber composite is subjected to a cyclic loading, the matrix surrounding the fiber-segment undergoes high cyclic shear strains, thus, producing significant viscoelastic energy loss. Shear stress concentration may also induce partial debonding at the fiber/matrix interface that would result in a slip between the fiber and the matrix and in accompanying frictional losses. Such a fiber/matrix debonding would, however, affect adversely the strength and stiffness of the composite. It is, thus, often argued that it may be desirable to have a strong interfacial bond so that slip at the interface would not occur. Thus, the most viable mechanism of enhanced dissipation appears to be the shear deformation in the matrix caused by shear stress concentration near the fiber ends. Based on the stress transfer mechanism between the fiber and the matrix, it is obvious that there are several microstructural parameters that might influence the shear stress distribution at the interface. The situation becomes further complicated when the interaction between neighboring fibers, in the composite laminate, is taken into account. As indicated earlier, the "*Force-Balance Approach*" is used in this presentation to predict the damping and stiffness for this class of materials.

The basic assumptions for the *"Force Balance Approach"*, as adopted in this paper, are:

- The structural element is composed of an individual round fiber surrounded by a cylindrical matrix, and is under a uniaxial tensile loading (Figure 1).
- Both the fiber and matrix are isotropic.
- The mechanical response of the matrix is linear viscoelastic.
- The fiber contributes, to a certain extent, to energy dissipation.
- There is a perfect bonding between the fiber and the matrix. Further, the fiber/matrix interface is assumed to have the same viscoelastic properties of the bulk matrix.
- The transfer of load between the fiber and the matrix depends upon the difference between the actual displacement at a point on the fiber/matrix interface and the displacement that would exist if the fiber were not present.

In the force-balance approach, the expression for the elastic stiffness of the short-fiber composite is derived from the average fiber stress as based upon using Cox's analytical model concerning fiber stress distribution /9/. Subsequently, the elastic-viscoelastic correspondence principle, e.g., Hashin /10/ and Haddad /11-13/, is used to obtain the expression for the complex modulus of the assumed linear viscoelastic composite laminate. This involves the replacement of the elastic moduli of the fiber, matrix and composite in the expressions resulting from the linear elastic analysis, with the corresponding viscoelastic moduli. In the case of sinusoidal loading, the expression for the complex modulus would involve both the storage modulus and the associated-with loss modulus.

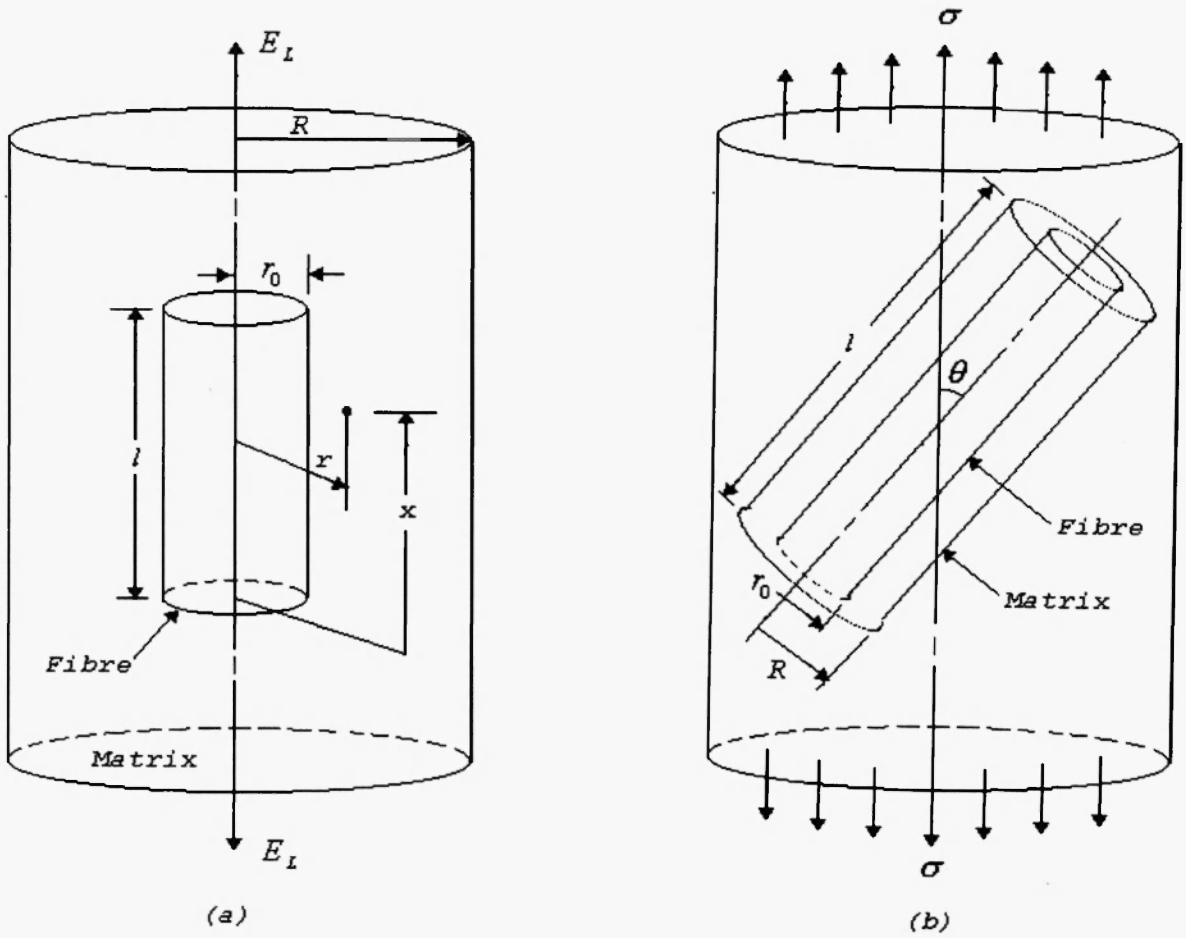

Fig. 1: Representative volume element: (a) Aligned case, (b) Off-axis case.

For a typical representative volume element, Figure 1, the expression of the modulus, E_x, of the composite along the loading axis may be expressed as, e.g., Agarwal and Broutman /14/,

$$\frac{1}{E_x} = \frac{\cos^4\theta}{E_L} + \frac{\sin^4\theta}{E_T} + \left(\frac{1}{G_{LT}} - \frac{2\nu_{LT}}{E_L}\right)\sin^2\theta\cos^2\theta \tag{1}$$

where E_L, E_T and G_{LT} are the longitudinal, transverse, and in-plane shear moduli, respectively. These moduli can be expressed, in the case of long-fiber composites, in terms of both the fiber and matrix material parameters, i.e., E_f, E_m, G_f, G_m, etc, and the fiber volume fraction V_f, by using, for instance, the rule-of-mixtures. For short-fiber composites, however, one cannot use the rule-of mixtures to represent the longitudinal modulus E_L. For short-fiber composites, the longitudinal modulus E_L depends also on the fiber aspect ratio, l/d. Based upon the shear-lag model (Cox /9/), the longitudinal modulus E_L may be expressed for the case of short-fiber composite by; see Feng /15/,

$$E_L = E_f\left(1-\frac{\tanh(\chi/2)}{(\chi/2)}\right)V_f + E_m(1-V_f) \tag{2}$$

where

$$\chi^2 = 8\frac{G_m}{E_f}\frac{(l/d)^2}{\ln(2R/d)} \tag{3}$$

The ratio R/d, where R is as illustrated in Figure 1 and d is the diameter of the fiber, is related to the fiber volume fraction V_f, for the particular packing array under consideration. For instance,

$$\left(\frac{R}{d}\right)^2 = \frac{\pi}{16V_f} \qquad \text{for a square array} \tag{4}$$

$$\left(\frac{R}{d}\right) = \frac{\pi}{8(3V_f)^{1/2}} \qquad \text{for a hexagonal array} \tag{5}$$

Based upon the work of Gibson *et al.* /3/, the packing geometry has an insignificant effect on the magnitude of damping. Therefore, we adopt, in the subsequent analysis, expression (4) corresponding to the square packing array. Combining, then, equations (3) and (4), it follows that

$$\chi^2 = 8\frac{G_m}{E_f}\frac{(l/d)^2}{\ln(\pi/4V_f)^{1/2}} \tag{6}$$

Equation (6) above shows that the parameter χ is essentially a function of fiber/matrix stiffness ratio E_f/G_m, fiber-aspect-ratio l/d, and fiber volume fraction V_f.

Meanwhile, the transverse modulus E_T and the transverse in-plane shear modulus G_{LT}, of the short- fiber composite may be considered as independent of fiber aspect ratio l/d. Therefore, one may adopt the formalism pertaining to long-fiber composites. In this context, we adopt here the following Halpin-Tsai expressions; see Agarwal and Broutman /14/,

$$E_T = E_m(1+2\eta_1 V_f)/(1-\eta_1 V_f) \tag{7}$$

$$G_{LT} = G_m(1+\eta_2 V_f)/(1-\eta_2 V_f) \tag{8}$$

where the coefficients η_1 and η_2 of the above two equations can be expressed, respectively, as

$$\eta_1 = [(E_f/E_m)-1]/[(E/E_m)+2] \tag{9}$$

$$\eta_2 = [(G_f / G_m) - 1][(G_f / G_m) + 1] \tag{10}$$

At the same time, the Poisson's ratio ν_{LT} of the short-fiber composite, that is assumed to be insensitive to fiber length, may be expressed, using a *'rule-of-mixture'* form, as

$$\nu_{LT} = \nu_f V_f + \nu_m (1 - V_f) \tag{11}$$

According to the previous assumptions, both fiber and matrix are considered to be linear viscoelastic materials. This permits us to use the elastic-viscoelastic correspondence principle to redefine the basic material properties within the realm of linear viscoelasticity. Thus, one has

$$\begin{aligned} E_x &= E_x^* = E_x' + iE_x'' \\ E_f &= E_f^* = E_f' + iE_f'' \\ E_m &- E_m^* - E_m' + iE_m'' \\ G_m &= G_m^* = G_m' + iG_m'' \end{aligned} \tag{12}$$

Here, the over-prime designates the storage modulus and the double over-prime identifies the loss modulus. Meantime, the damping (loss) factor is defined as the ratio between the loss modulus and the storage modulus, i.e.,

$$\begin{aligned} \eta_c &= E_x'' / E_x' \\ \eta_f &= E_f'' / E_f' \\ \eta_m &= E_m'' / E_m' \\ \eta_{Gm} &= G_m'' / G_m' \end{aligned} \tag{13}$$

Upon using Eq. (12), equations (2), (7) and (8) may be written, respectively, as

$$E_L^* = (E_f' + iE_f'')\left[1 - \frac{\tanh(\chi^* / 2)}{(\chi^* / 2)}\right] V_f + (E_m' + iE_m'')(1 - V_f) \tag{14}$$

$$E_T^* = (E_m' + iE_m'')\frac{1 + 2\eta_1^* V_f}{1 - \eta_1^* V_f} \tag{15}$$

$$G_{LT}^* = (G_m' + iG_m'')\frac{1 + \eta_2^* V_f}{1 - \eta_2^* V_f} \tag{16}$$

where

$$\left(\chi^*\right)^2 = 8\frac{(G'_m + iG''_m)(l/d)^2}{(E'_f + iE''_f)\ln(\pi/4V_f)^{1/2}} \tag{17}$$

$$\eta_1^* = \frac{[(E'_f + iE''_f)/(E'_m + iE''_m)] - 1}{[(E'_f + iE''_f)/(E'_m + iE''_m)] + 2} \tag{18}$$

$$\eta_2^* = \frac{[(G'_f + iG''_f)/(G'_m + iG''_m)] - 1}{[(G'_f + iG''_f)/(G'_m + iG''_m)] + 1} \tag{19}$$

Substituting E_L^*, E_T^* and G_{LT}^* from equations (14) to (16) for E_L, E_T and G_{LT}, respectively, into Eq. (1), and also E_x^* for E_x into the same equation, it follows that

$$\frac{1}{E'_x + iE''_x} = \frac{\cos^4\theta}{E_L^*} + \frac{\sin^4\theta}{E_T^*} + \left(\frac{1}{G_{LT}^*} - \frac{2\nu_{LT}}{E_L^*}\right)\sin^2\theta\cos^2\theta \tag{20}$$

Equation (20), above, can then be solved by separating its real and imaginary parts to determine E'_x and E''_x for the composite.

Since the loss moduli are generally small, one may neglect the higher order terms of loss factors such as η_f^2 and $\eta_{Gm}\eta_f$. Subsequently, one may obtain the following expression by combining the above-mentioned set of equations (17) to (19).

$$\frac{\chi^*}{2} = \frac{\chi}{2}\left[1 + \frac{1}{2}i\left(\eta_{Gm} - \eta_f\right)\right] \tag{21}$$

Further, one may use a Taylor's series approximation and similarly neglect any resulting higher order terms in the loss factors to obtain

$$\tanh\frac{\chi^*}{2} = \tanh\frac{\chi}{2} + i\frac{\chi}{4}\frac{(\eta_{Gm} - \eta_f)}{\cosh^2(\chi/2)} \tag{22}$$

Thus, by combining equations (14) to (22), one determines analytical representations of E'_x, E''_x and η_x.

Among the many microstructural parameters, of the dealt with composite laminate, that may be considered for the optimization process, we narrowed down our attention to three parameters, namely, θ, V_f and l/d, representing, respectively, the fiber off-axis angle with respect to the longitudinal axis x of the laminate (the loading direction), the fiber volume fraction and the fiber aspect ratio. While the optimization

model is presented below in a generalized manner, the particular case of E-glass/epoxy composite, Table 1, is being dealt with as an illustration.

For a large class of composite materials used in industry, the fiber volume fraction varies within the range of 50% to 70%. Meanwhile, the observation made by Cox /9/ shows that, for short-fiber reinforced composite materials, the reduction of the effective longitudinal modulus due to the load transfer from fiber to fiber is considered significant only for fiber aspect ratios, l/d, less than 100. Therefore, one could set the fiber volume fraction to vary within the range from 50% to 70% and the fiber-aspect-ratio to vary within the range from 1 to 100.

Table 1

Selected material properties of Scotchply 1002 matrix epoxy and E-glass fibers at room temperature; adapted after Gibson and Plunkett /16/.

Material Properties	Epoxy	E-glass
Young's modulus GPa	3.79	72.40
Shear modulus GPa	1.38	30.30
Damping factor	0.015	0.0014
Shear damping factor	0.018	0.0014
Poisson's ratio, ν	0.36	0.2
Specific gravity, g	1.23	2.54

Figures 2 to 6 are obtained by setting, respectively, the fibre of-axis angle θ as 0°, 40°, 60°, 80° and 90°, and plotting the ratios η_x / η_m and E'_x / E'_m against the fibre volume fraction V_f and the fibre aspect ratio l/d. In these figures, it is clear that with the increase of fibre off-axis angle, the values of the ratio η_x / η_m are increasing, while those for E'_x / E'_m are decreasing. When the fibre off-axis angle reaches a value between 40° to 60°, both η_x / η_m and E'_x / E'_m curves change their directions, which demonstrate that for a fibre off-axis angle θ within the range of 40° to 60°, both the ratios η_x / η_m and E'_x / E'_m reach their extreme values (maximum and minimum, respectively) almost simultaneously.

Figures 7 to 11, which are plotted by setting the fibre aspect ratio l/d as 5, 20, 40, 80 and 100, respectively, present the ratios η_x / η_m and E'_x / E'_m against the fibre volume fraction V_f and the fibre off-axis angle θ. In these figures, one observes that the value η_x / η_m decreases monotonously as the fibre aspect ratio l/d increases and for value of $l/d > 15$, the rate of decrease in value slows down until the fibre aspect ratio l/d reaches 20, whereby the value of the ratio η_x / η_m maintains a constant value afterwards. The ratio E'_x / E'_m also increases sharply until the fibre aspect ratio l/d reaches a value of about 20. With the fibre-aspect-ratio ranging from 20 to 60, the ratio E'_x / E'_m increases slowly with the increase of the fibre-aspect-ratio l/d and seems to have a constant value from $l/d = 60$ upwards.

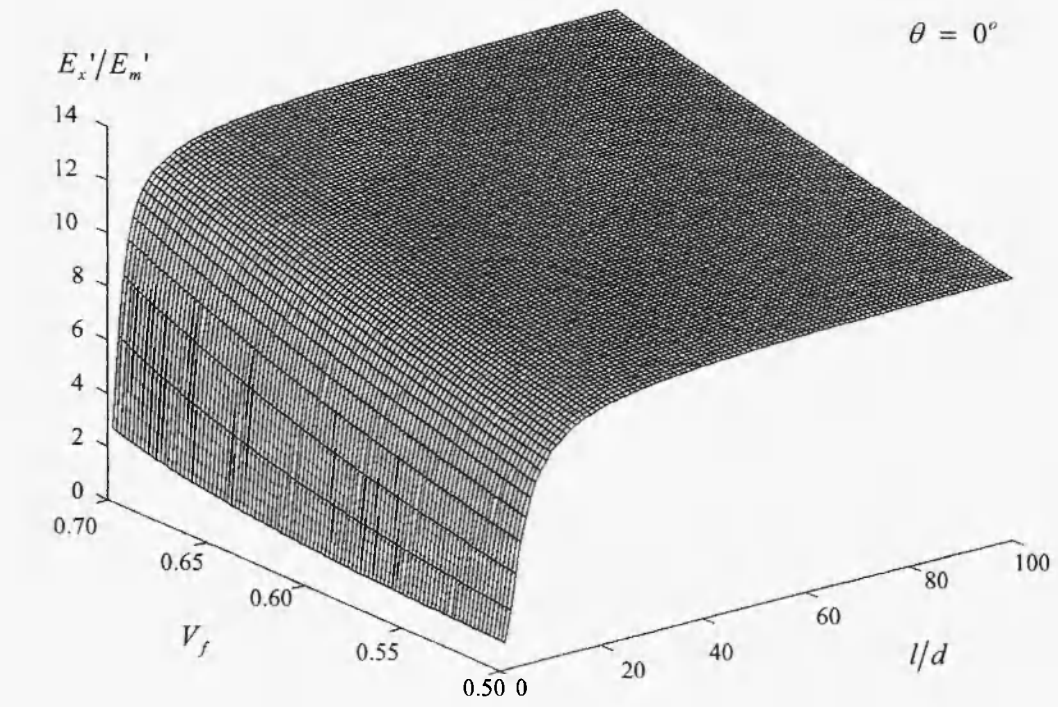

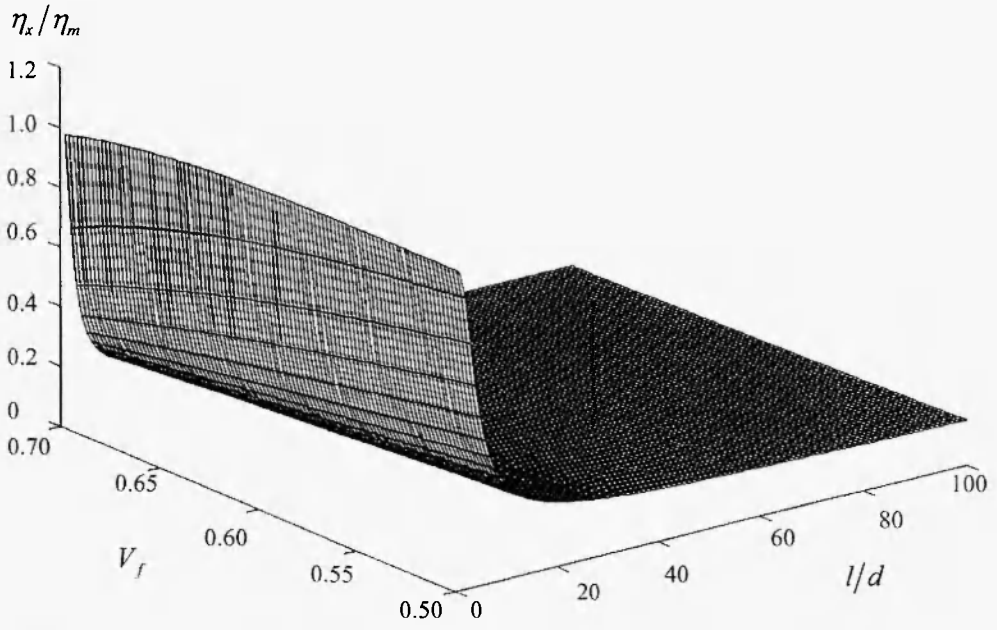

Fig. 2: Non-dimensional ratios E_x'/E_m' and η_x/η_m vs. fiber volume fraction V_f and fiber aspect ratio l/d. Off-axis angle θ of desired composite materials, with material properties of each component as shown in Table 1, is set to be 0°.

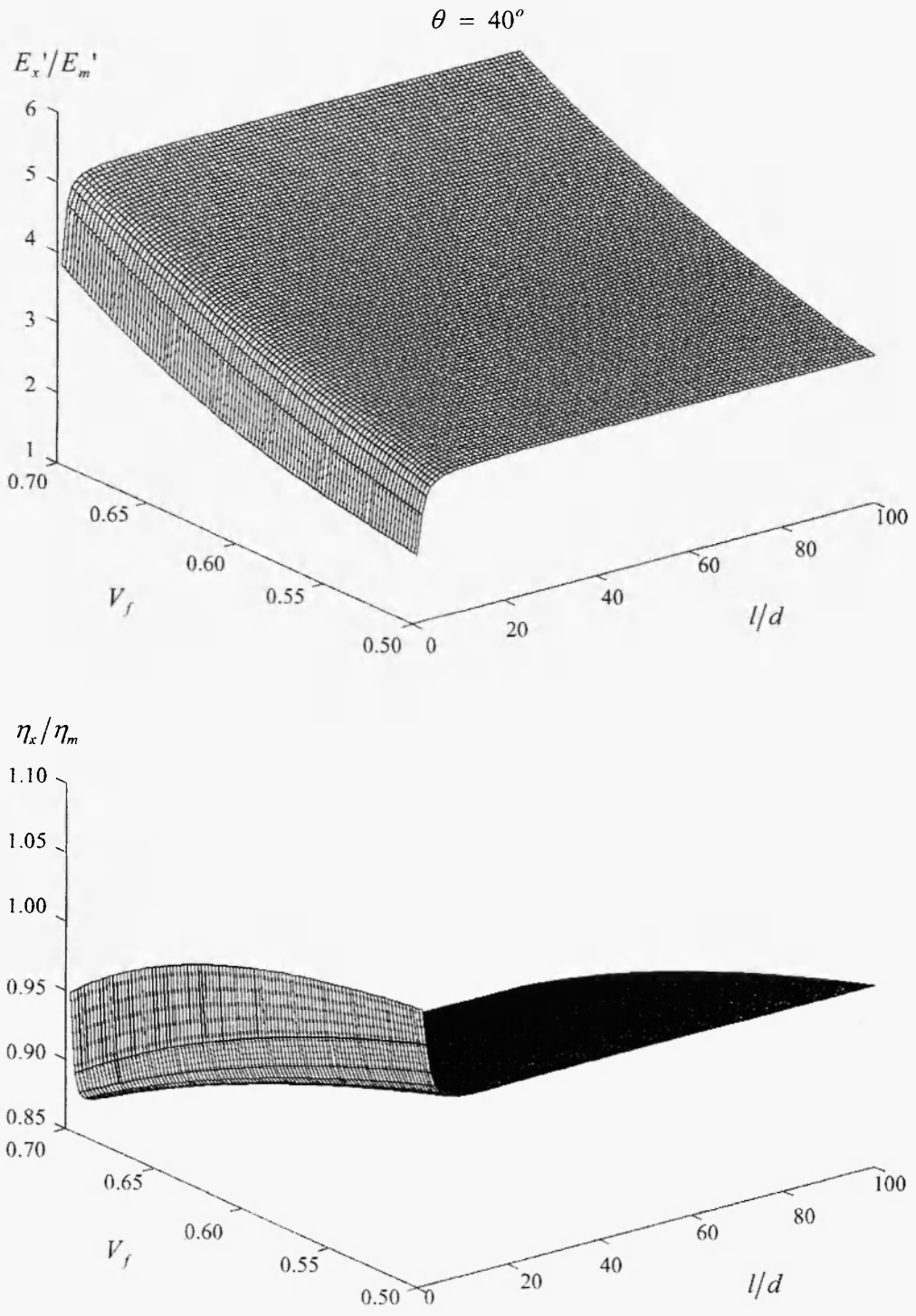

Fig. 3: Non-dimensional ratios E_x' / E_m' and η_x / η_m vs. fiber volume fraction V_f and fiber aspect ratio l/d. Off-axis angle θ of desired composite materials, with material properties of each component as shown in Table 1, is set to be 40°.

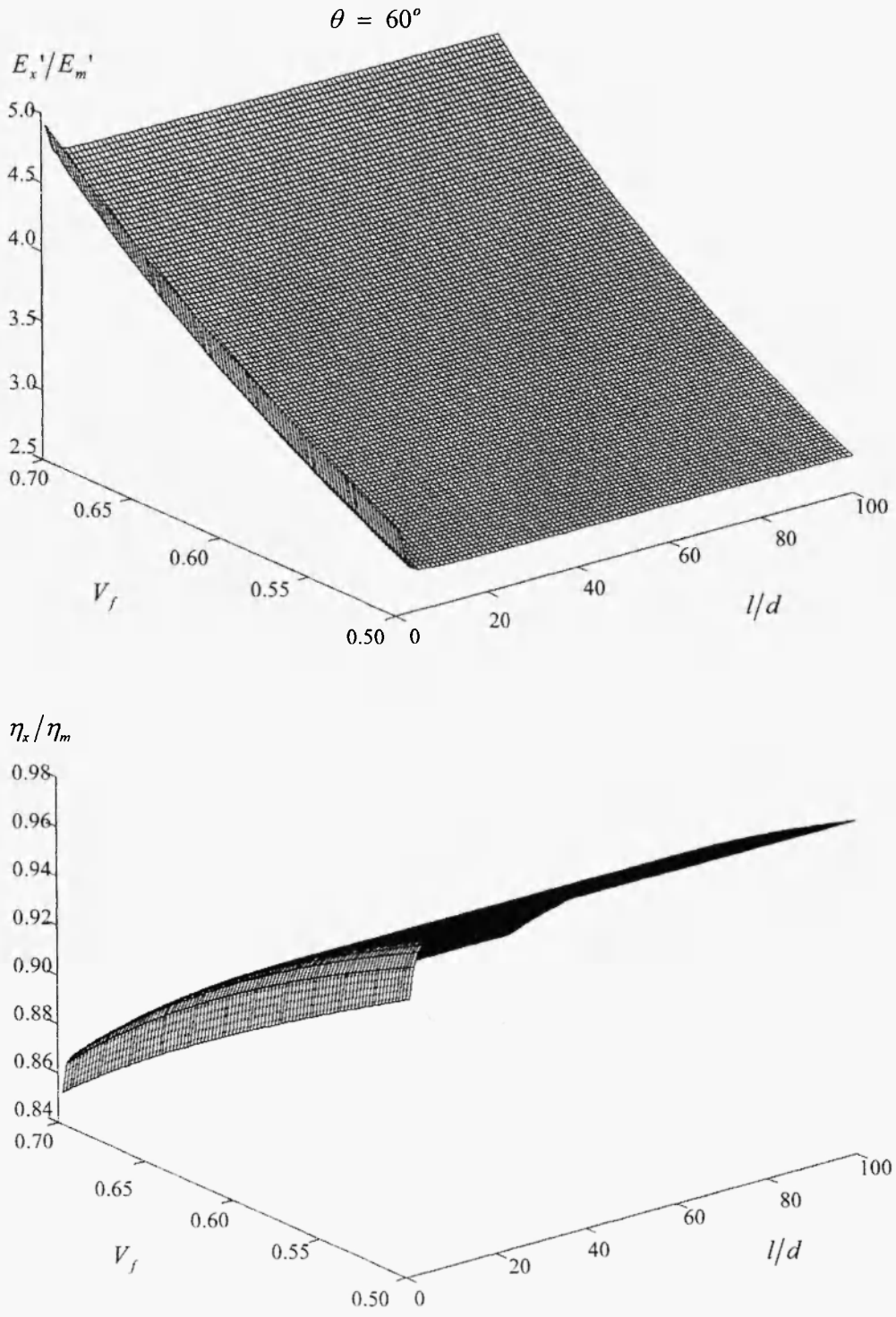

Fig. 4: Non-dimensional ratios E_x'/E_m' and η_x/η_m vs. fiber volume fraction V_f and fiber aspect ratio l/d. Off-axis angle θ of desired composite materials, with material properties of each component as shown in Table 1, is set to be 60°.

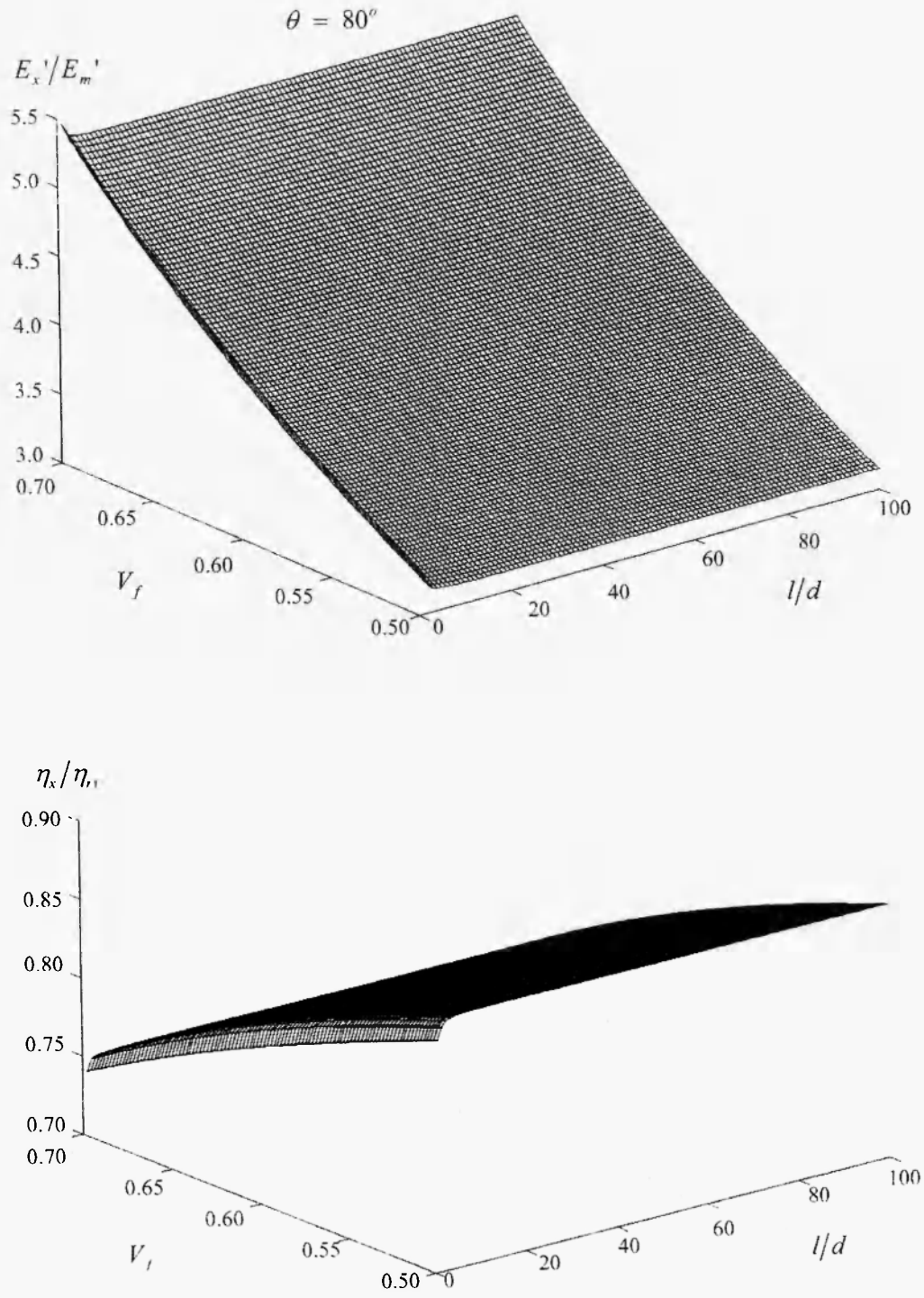

Fig. 5: Non-dimensional ratios E_x' / E_m' and η_x / η_m vs. fiber volume fraction V_f and fiber aspect ratio l/d. Off-axis angle θ of desired composite materials, with material properties of each component as shown in Table 1, is set to be 80°.

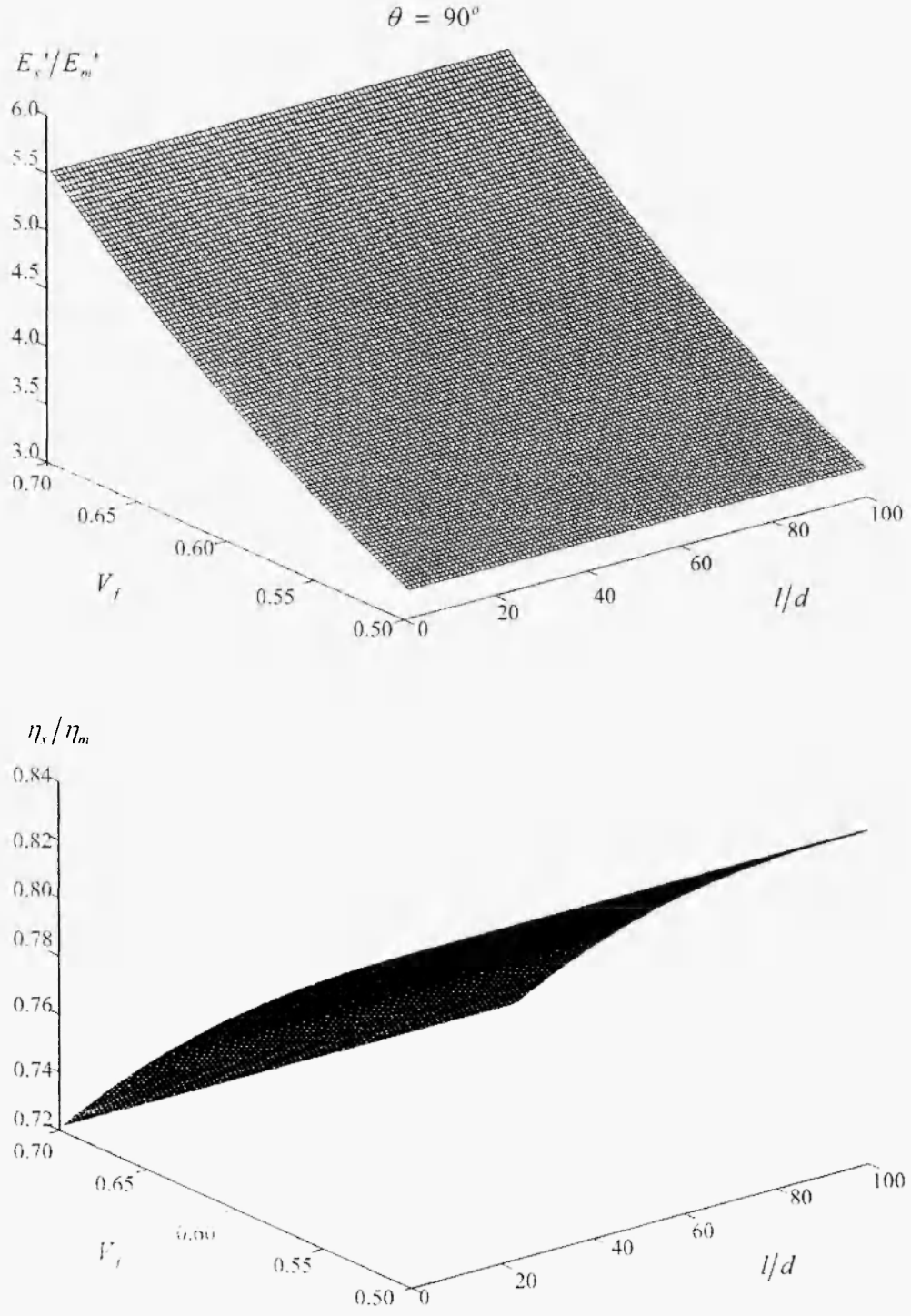

Fig. 6: Non-dimensional ratios E_x' / E_m' and η_x / η_m vs. fiber volume fraction V_f and fiber aspect ratio l/d. Off-axis angle θ of desired composite materials, with material properties of each component as shown in Table 1, is set to be 90°.

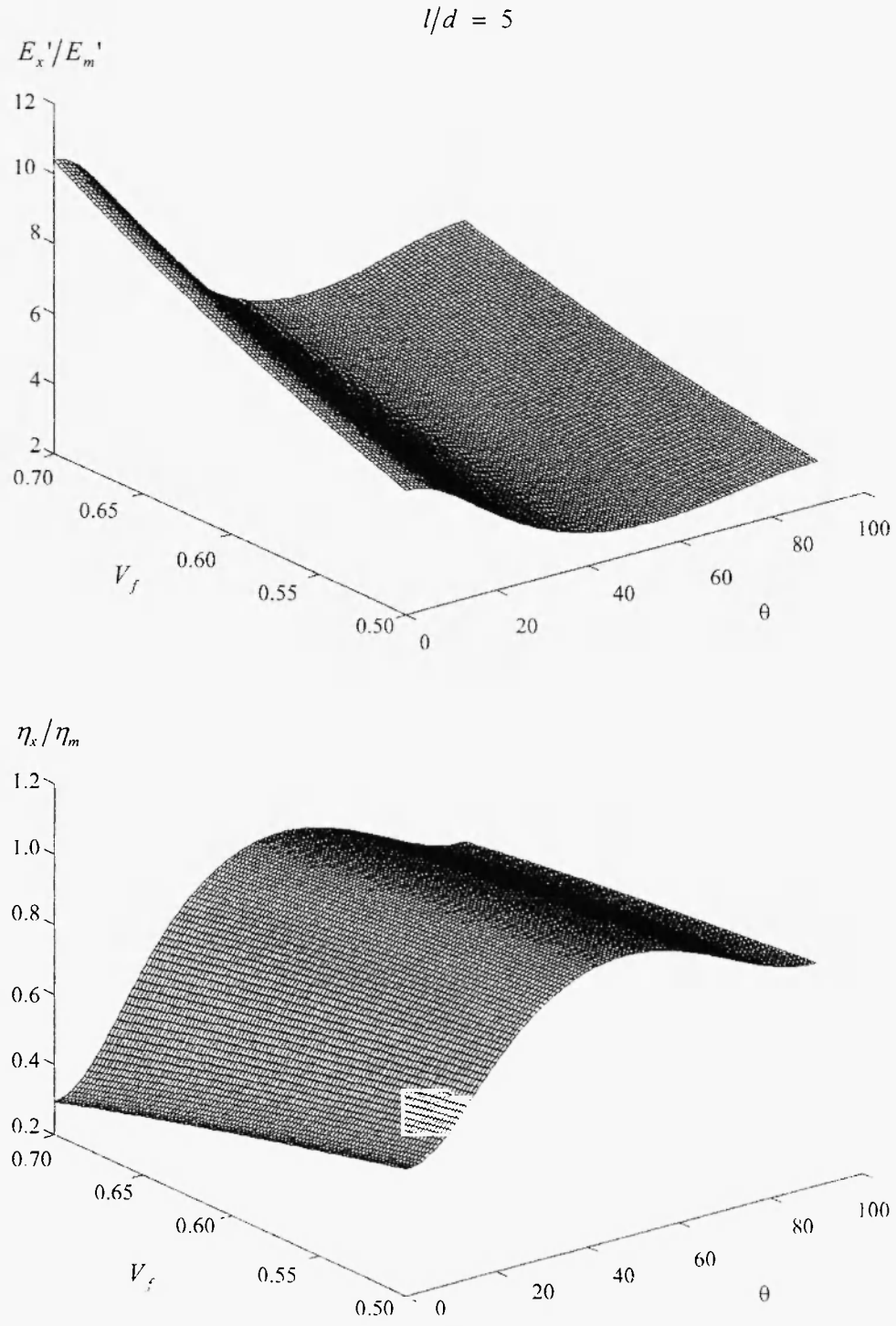

Fig. 7: Non-dimensional ratios E_x' / E_m' and η_x / η_m vs. fiber volume fraction V_f and off-axis angle θ. Fiber aspect ratio l/d of desired composite materials, with material properties of each component as shown in Table 1, is set to be 5.

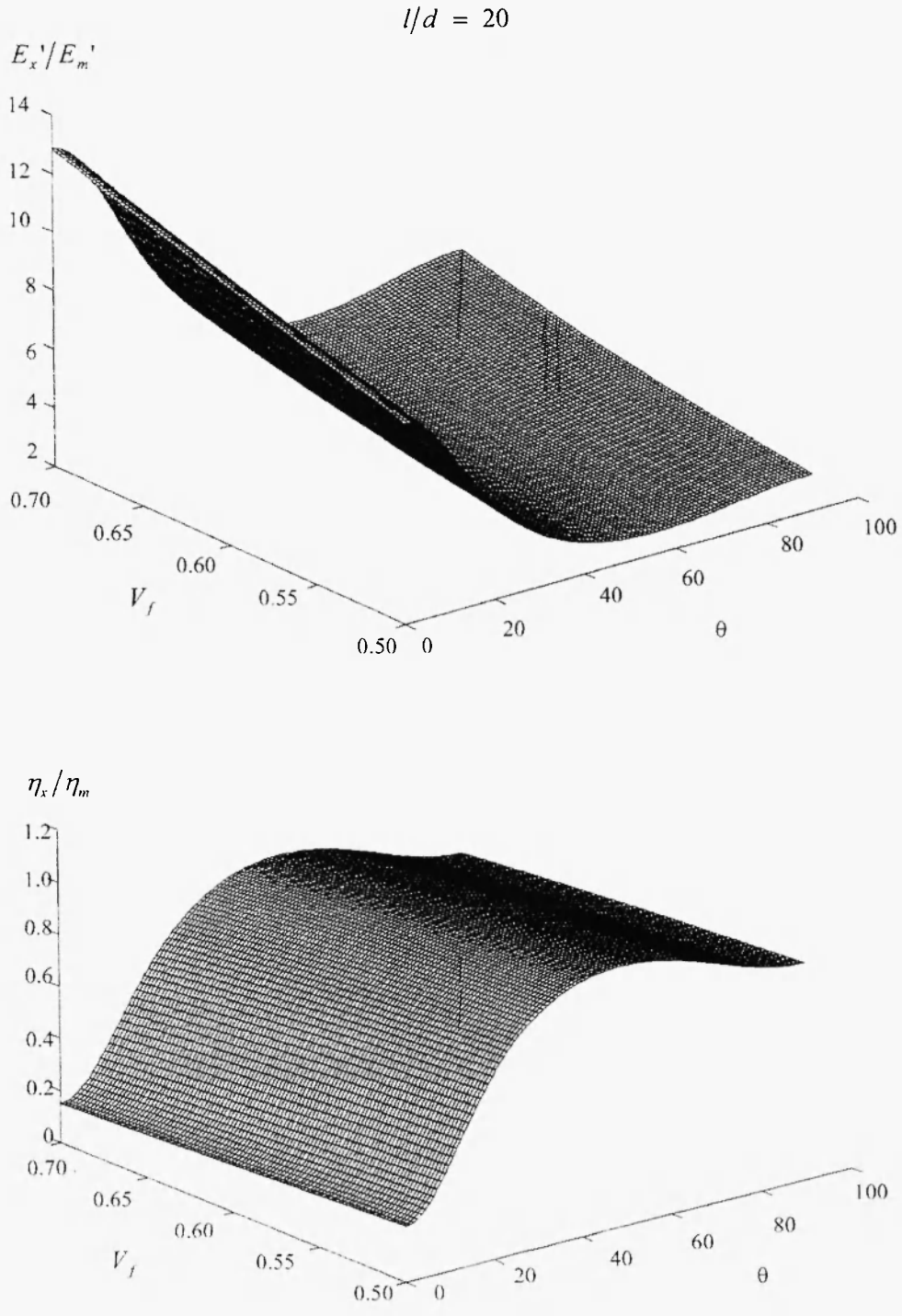

Fig. 8: Non-dimensional ratios E_x' / E_m' and η_x / η_m vs. fiber volume fraction V_f and off-axis angle θ. Fiber aspect ratio l/d of desired composite materials, with material properties of each component as shown in Table 1, is set to be 20.

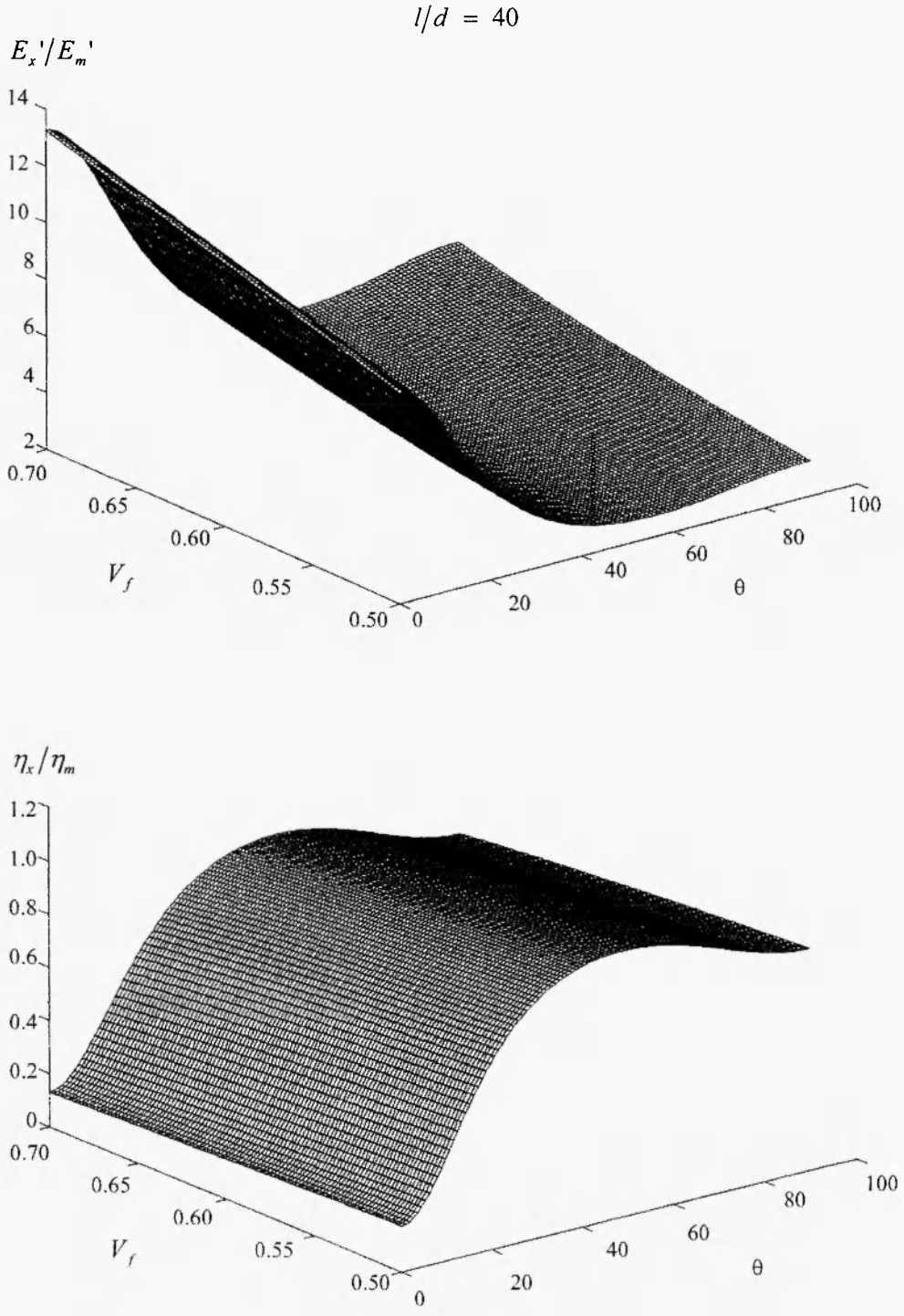

Fig. 9: Non-dimensional ratios E_x' / E_m' and η_x / η_m vs. fiber volume fraction V_f and off-axis angle θ. Fiber aspect ratio l/d of desired composite materials, with material properties of each component as shown in Table 1, is set to be 40.

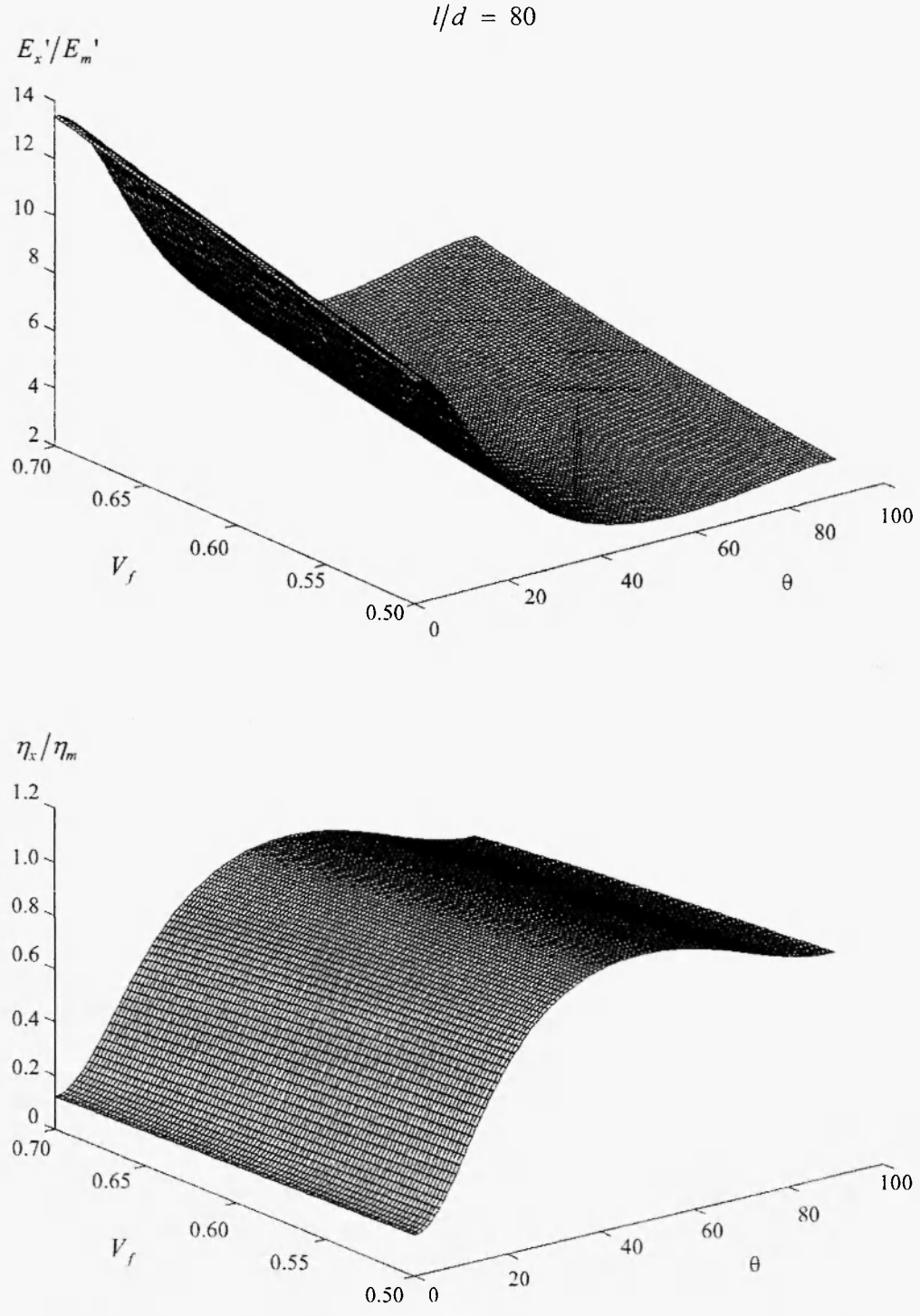

Fig. 10: Non-dimensional ratios E_x'/E_m' and η_x/η_m vs. fiber volume fraction V_f and off-axis angle θ. Fiber aspect ratio l/d of desired composite materials, with material properties of each component as shown in Table 1, is set to be 80.

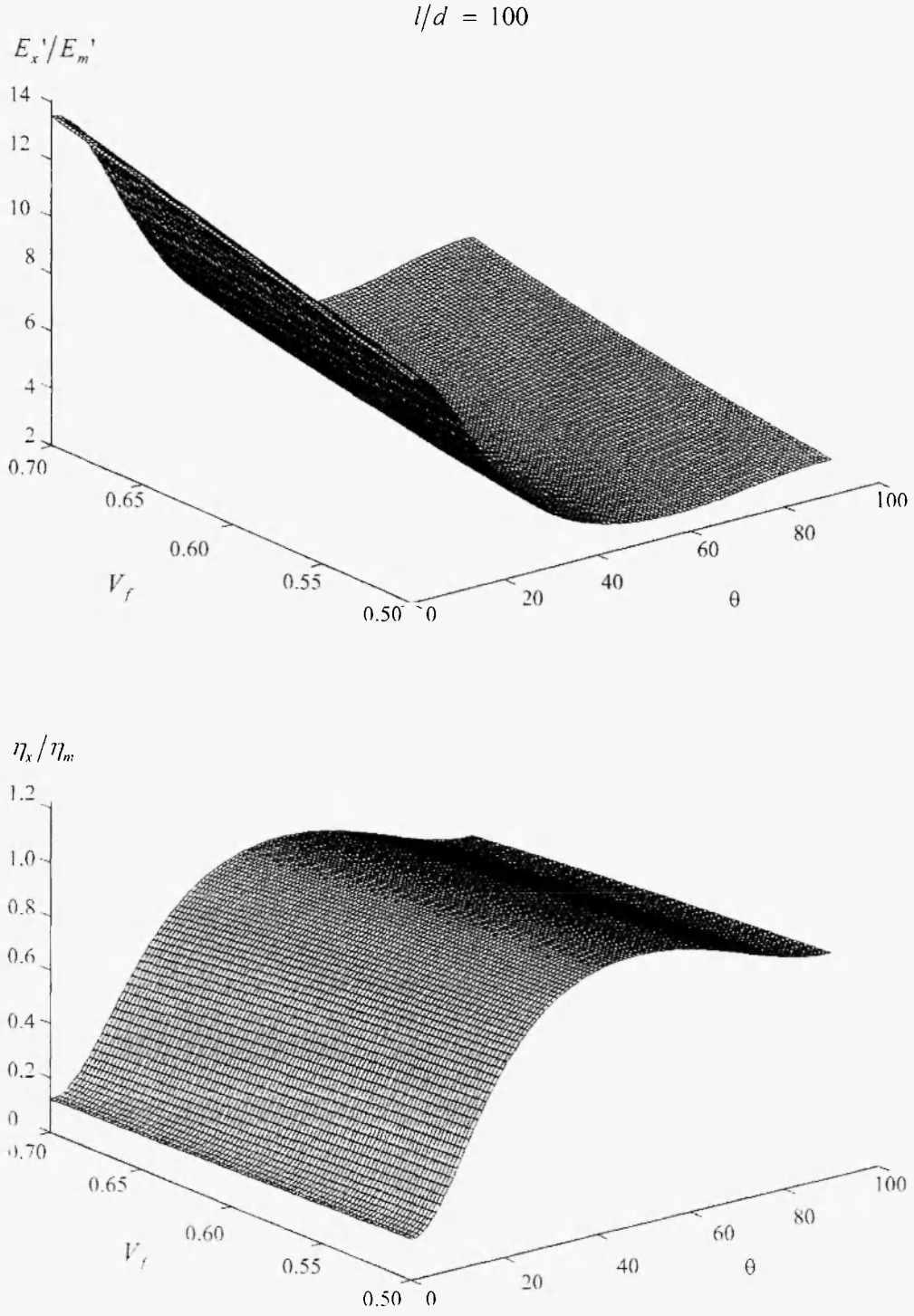

Fig. 11: Non-dimensional ratios E'_x / E'_m and η_x / η_m vs. fiber volume fraction V_f and off-axis angle θ. Fiber aspect ratio l/d of desired composite materials, with material properties of each component as shown in Table 1, is set to be 100.

By setting the fibre volume fraction V_f at 50%, 60% and 70%, the ratios η_x / η_m and E'_x / E'_m against the fibre aspect ratio l/d and the fibre off-axis angle θ are plotted as shown in Figures 12 to 14. In these figures, one can identify that with the increase of the fibre volume fraction, both the ratios η_x / η_m and E'_x / E'_m change almost linearly, with the values of the ratio η_x / η_m are monotonously decreasing and those for E'_x / E'_m are monotonously increasing.

It is apparent from the obtained results that among the three considered independent variables, the fibre off-axis angle θ has the most significant influence on the damping and stiffness of short fibre-reinforced composites. The obtained numerical results appear to be in good agreement with the observations made by Gibson *et al.* /3/, Sun *et al.* /4/, and Suarez *et al.* /5/.

3. OPTIMIZATION

From the above numerical results, one can observe that in order to increase the damping of a short-fibre-reinforced composite, it is necessary to sacrifice the stiffness of this material. The analysis of the trade-off between damping and stiffness will gain more and more attention from researchers and design engineers, due to the high-volume use of composite materials in both aerospace and automotive industries. Therefore, the simultaneous optimization of these two properties for the design of high performance short-fibre reinforced composite structures becomes remarkably important in the development of structural materials and structural dynamics technology. As it is well recognized, one of the most important advantages of a fibre-reinforced composite material over its metallic counterparts is its light specific weight. Thus, it is necessary to include this property in the dealt-with optimization problem. Thus, the optimization problem will involve the maximization of both damping and stiffness and, on the other hand, minimization of the composite specific weight. That is, *three* objective functions are involved in the optimization problem. In this context, the "*inverted utility function method*", e.g., Rao /17/, is adopted in this research to deal with this multi-objectives optimization problem.

3.1 The Inverted Utility Function Method

In this method, a utility function U_i (f_i) is defined for each objective function as

$$U_i = -w_i f_i(X) \tag{23}$$

where $f_i(X)$, the ith objective function, with weighing factor as w_i (i=1,2, ...,k), is to be minimized. In the process of optimization, one inverts each utility function and attempts to minimize or reduce the total undesirability, whereby

$$U^{-1} = \sum_{i=1}^{k} U_i^{-1} = \sum_{i=1}^{k} \left(\frac{1}{U_i} \right) = \sum_{i=1}^{k} -\frac{1}{w_i} \frac{1}{f_i(X)} = \sum_{i=1}^{k} -a_i \left(\frac{1}{f_i(X)} \right) \tag{24}$$

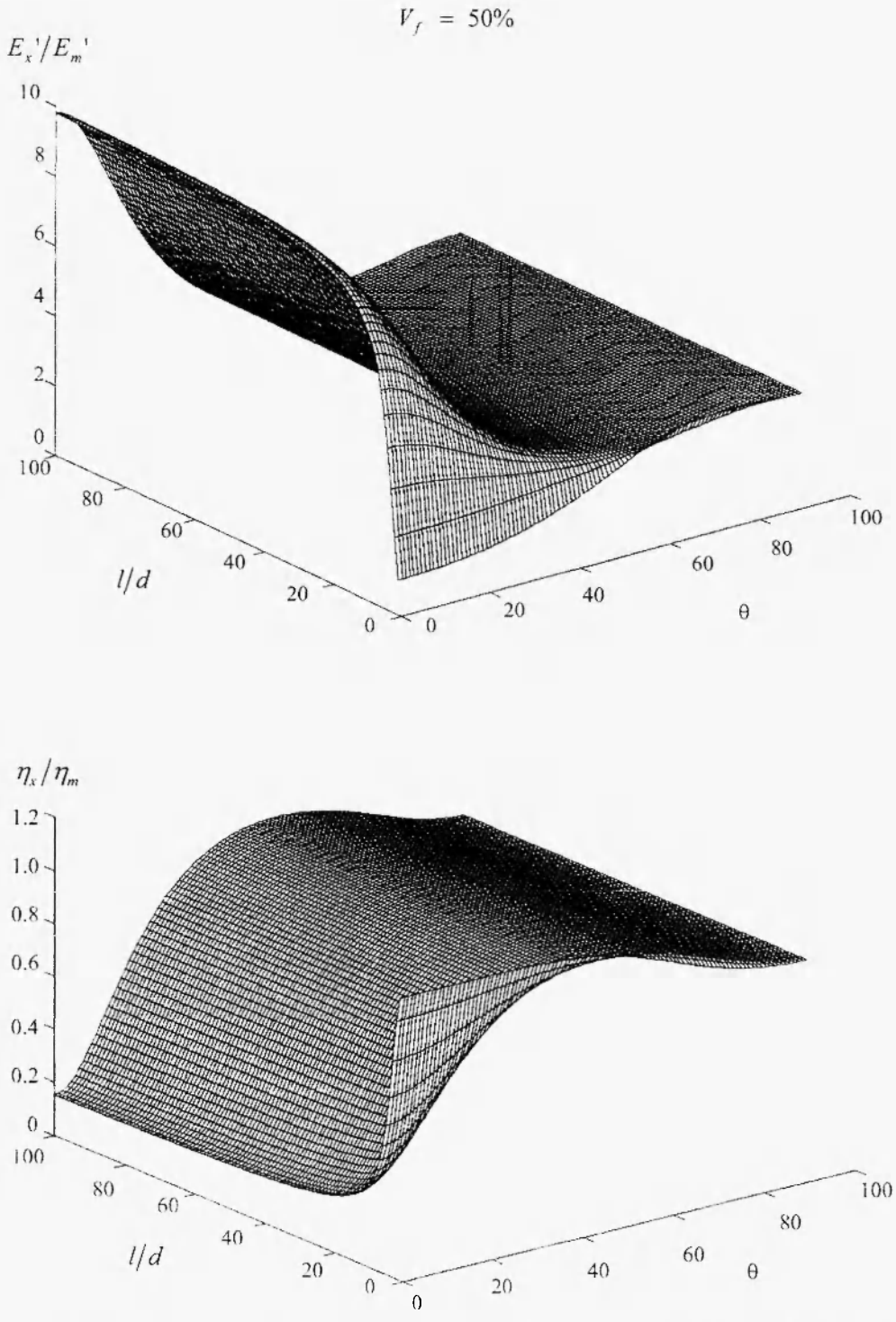

Fig. 12: Non-dimensional ratios E_x'/E_m' and η_x/η_m vs. fiber aspect ratio l/d and off-axis angle θ. Fiber volume fraction V_f of desired composite materials, with material properties of each component as shown in Table 1, is set to be 50%.

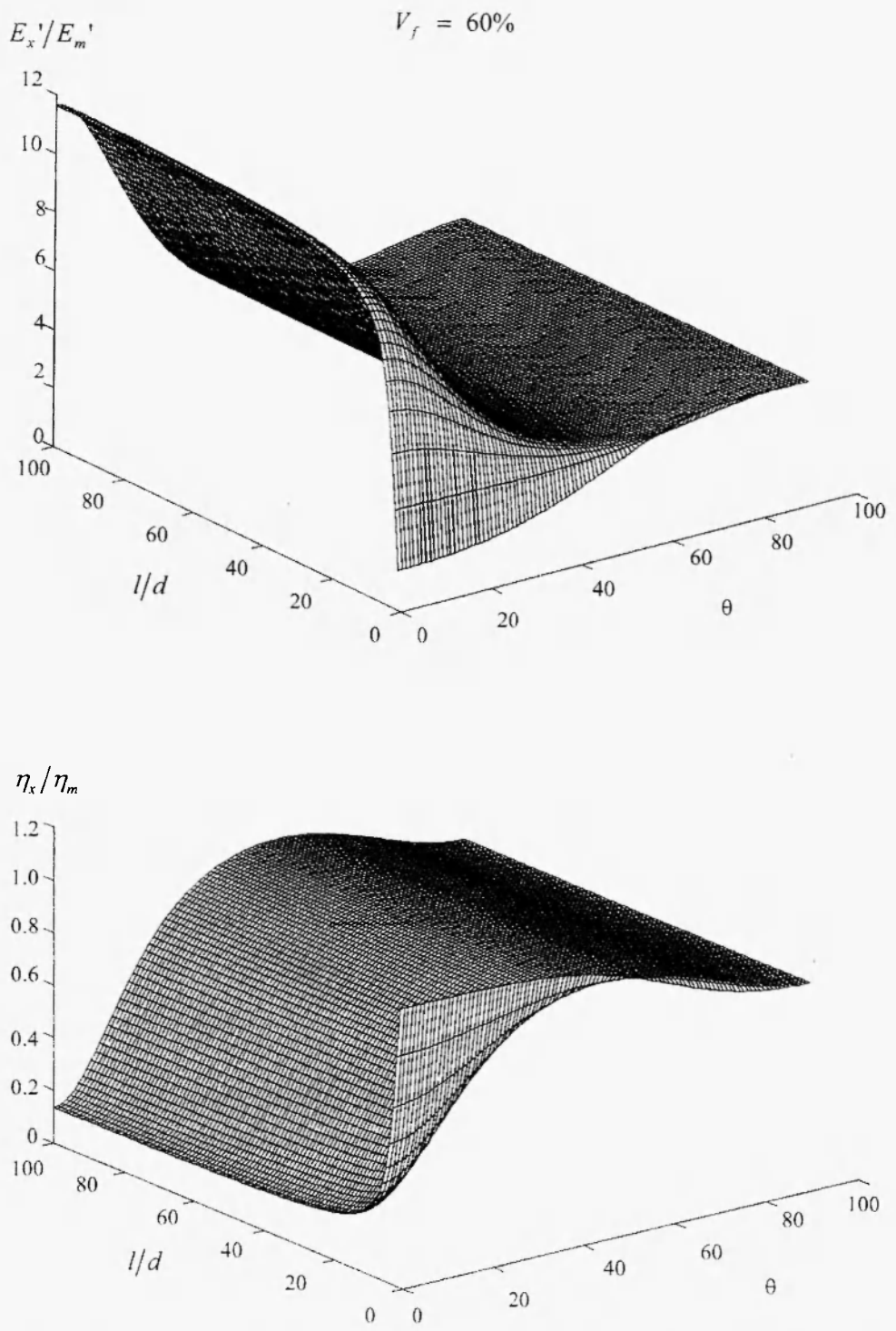

Fig. 13: Non-dimensional ratios E_x' / E_m' and η_x / η_m vs. fiber aspect ratio l/d and off-axis angle θ. Fiber volume fraction V_f of desired composite materials, with material properties of each component as shown in Table 1, is set to be 60%.

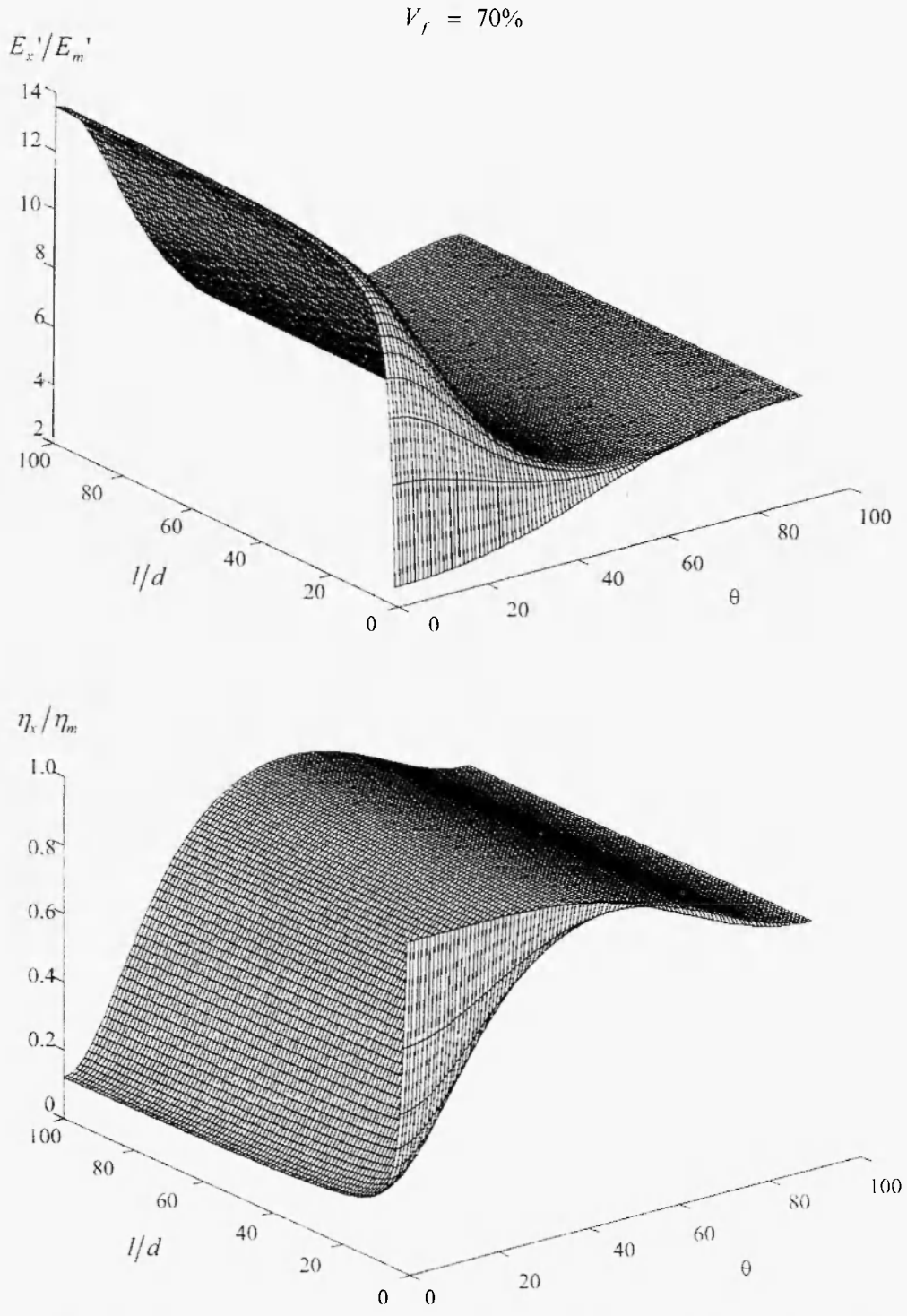

Fig. 14: Non-dimensional ratios E_x'/E_m' and η_x/η_m vs. fiber aspect ratio l/d and off-axis angle θ. Fiber volume fraction V_f of desired composite materials, with material properties of each component as shown in Table 1, is set to be 70%.

in which the scalar weighing factors a_i are defined by

$$a_i = \frac{1}{w_i}; \quad \sum_{i=1}^{k} a_i = 1$$

Thus, in this paper, the solution of the optimization problem is established by minimizing U_i^{-1} subject to the imposed constraints. In this, the selection of the magnitudes of the scalar weighing factors a_i would depend on the importance of each objective function to the overall optimization problem.

3.2. Multivariable Non-linear Optimization

In the present work, the corresponding utility functions of each objective function are set as

$$U_1 = w_1\left(\frac{\eta_x}{\eta_m}\right) \tag{25}$$

$$U_2 = w_2\left(\frac{E'_x}{E'_m}\right) \tag{26}$$

$$U_3 = -w_3\left(\frac{\bar{W}}{\bar{W}_m}\right) \tag{27}$$

where $\bar{W}$ is the specific weight for the dealt-with short-fiber reinforced composite, which is defined in terms of the fiber volume fraction V_f as

$$\bar{W} = \bar{W}_f V_f + \bar{W}_m (1 - V_f) \tag{28}$$

In equations (25) to (28) above, $\bar{W}_f$, $\bar{W}_m$, E'_m and η_m are set in accordance with the material properties of the considered E-glass/epoxy short-fiber reinforced composite (Table 1).

Substituting equations (25) to (27) into Eq. (24), the total undesirability of this design problem becomes

$$U^{-1} = a_1\left(\frac{\eta_m}{\eta_x}\right) + a_2\left(\frac{E'_m}{E'_x}\right) + a_3\left(\frac{\bar{W}_m}{\bar{W}}\right) \tag{29}$$

In the present optimization problem, both damping and stiffness are considered to be of about the same importance; meantime, each is of more significance, to the optimization problem than the specific weight. Thus, in this paper, the weighing factors are taken as $a_1 = 0.513$, $a_2 = 0.387$ and $a_3 = 0.1$. Further, for the

reasons stated earlier in the paper, the constraints for the optimization problem are set as

$$\begin{aligned} &0.5 < V_f \leq 0.7 \\ &1 < l/d \leq 100 \\ &0^o \leq \theta < 90^o \end{aligned} \tag{30}$$

3.3 Implementation of Non-Linear Programming

The optimization of this design work takes now the following format:

$$\begin{aligned} &\text{Minimize} && U^{-1} \\ &\text{Subject to} && 0.5 < V_f < 0.7 \\ & && 1 \leq l/d \leq 100 \\ & && 0^o \leq \theta \leq 90^o \end{aligned} \tag{31}$$

This is a typical constrained non-linear optimization problem. In order to simplify this problem, one can adopt the mapping technique (variable transformation technique) to deal with the parametric constraints referred to above, e.g., Rao /17/. By using this technique, the constrained optimization problem could be solved by a non-constrained optimization technique.

In the mapping technique, one assumes that there is a minimization problem $f(X)$ where $X^T = [x_j]$ with the parametric constraints set as

$$l_i < x_i < u_i \tag{32}$$

with $j = 1, 2, 3, ..., n$; $i = 1, 2, 3, ..., m$.

In this context, one can use the general mapping procedure as

$$x_i = l_i + (u_i - l_i)\sin^2 y_i \tag{33}$$

Therefore, the objective function $f(X)$ changes to $f(X^*, Y)$, where $Y^T = [y_i]$ and X^* would include all the components of variable vector X except x_i. If $m = n$, $f(X^*, Y)$ becomes $f(Y)$.

In this context, the mapping procedure can thus be utilized based upon the above-mentioned parametric constraints, Eq. (31), as

$$\begin{aligned} \theta &= 90^{o}\sin^{2}y_1 \\ l/d &= 1+99\sin^{2}y_2 \\ V_f &= 0.5+0.2\sin^{2}y_3 \end{aligned} \tag{34}$$

where $Y^T=[y^1,y^2,y^3]$ represent the mapping variables in the dealt with procedure. Therefore, one can convert this constrained non-linear optimization problem $U^{-1}(\theta, l/d, V_f)$, as Eq. (31), to non-constrained non-linear optimization $U^{-1}(y_1, y_2, y_3)$ and solve this problem by using a non-constrained optimization technique.

The "Simplex Method", see Rao /17/, seems to be suitable for this non-constrained non-linear optimization problem with a relatively small number of variables. In the referred-to method, the movement of the "Simplex" of n+1 points in n-dimensional space towards an optimal point is achieved by using three operations known as the "*Reflection*", "*Contraction*" and "*Expansion*" techniques.

Following the algorithm of the "Simplex Method", we implement a Fortran program to solve this optimization problem (see Fig. 15 for the pertaining flowchart).

Before running the Fortran program, we have to set a few parameters, namely, a starting point, desired accuracy of this problem, and a probe length which are used to construct the initial "Simplex", as well as "Reflection", "Expansion" and "Contraction" coefficients, as shown in the "Simplex" flowchart (Fig. 15). By setting the starting point as $X^T=[0,0,0]$, the accuracy of this problem as $ACCUR=0.001$, the probe length, which is used to construct the initial "Simplex", as $PLE=0.1$, the "Reflection" coefficient as $A=1.0$, the "Expansion" coefficient as $Y=2.0$, and the "Contraction" coefficient as $B=0.5$, the final result is given out as: the optimal fibre off-axis angle $\theta=44.4°$, the optimal fibre volume fraction $V_f=60.60\%$ and the fibre aspect ratio $l/d=1.50$.

These results are in good agreement with the observations made, for instance, by Sun and Gibson /4/ that for small off-axis angles θ (say $\theta<45°$), η_x becomes maximum in the whisker or microfiber composites range (i.e. for very small l/d, say $l/d<5$) and the stiffness E_x' for microfiber and whisker composites is also relatively high. Therefore, in order to achieve high stiffness E_x' and high damping η_x, microfiber and whisker composites seem to be the ideal candidates. There is no comment available, in the searched references, on the influence of fiber volume fraction V_f on the damping, stiffness and specific weight.

If the starting points, Y^T, are set at various points within the range from [0,0,0] to [95,95,95] and with the various increments (0.5 or 5.0), and the same input parameters that were used in the above case, one could get outputs as shown in Table 2. In this case, it is obvious that we get multiple local minima. For each case of these local minima, the off-axis angle remains almost the same, i.e., approximately 43.75°, and fiber volume fraction and fiber aspect ratio change in opposite directions and could be catalogued into two groups, i.e., ($l/d\approx1.38$, $V_f\approx62\%$) and ($l/d\approx85$, $V_f\approx54\%$). It is obvious that this interesting observation gives more flexibility in the design of high performance fiber reinforced composites by using fibers with either lower fiber aspect ratio, i.e., $l/d\approx1.38$ and relatively higher fiber volume fraction, i.e., $V_f\approx62\%$, or a higher fiber-aspect-ratio, i.e., $l/d\sim85$ and relatively a lower fiber volume fraction, i.e., $V_f\approx54\%$.

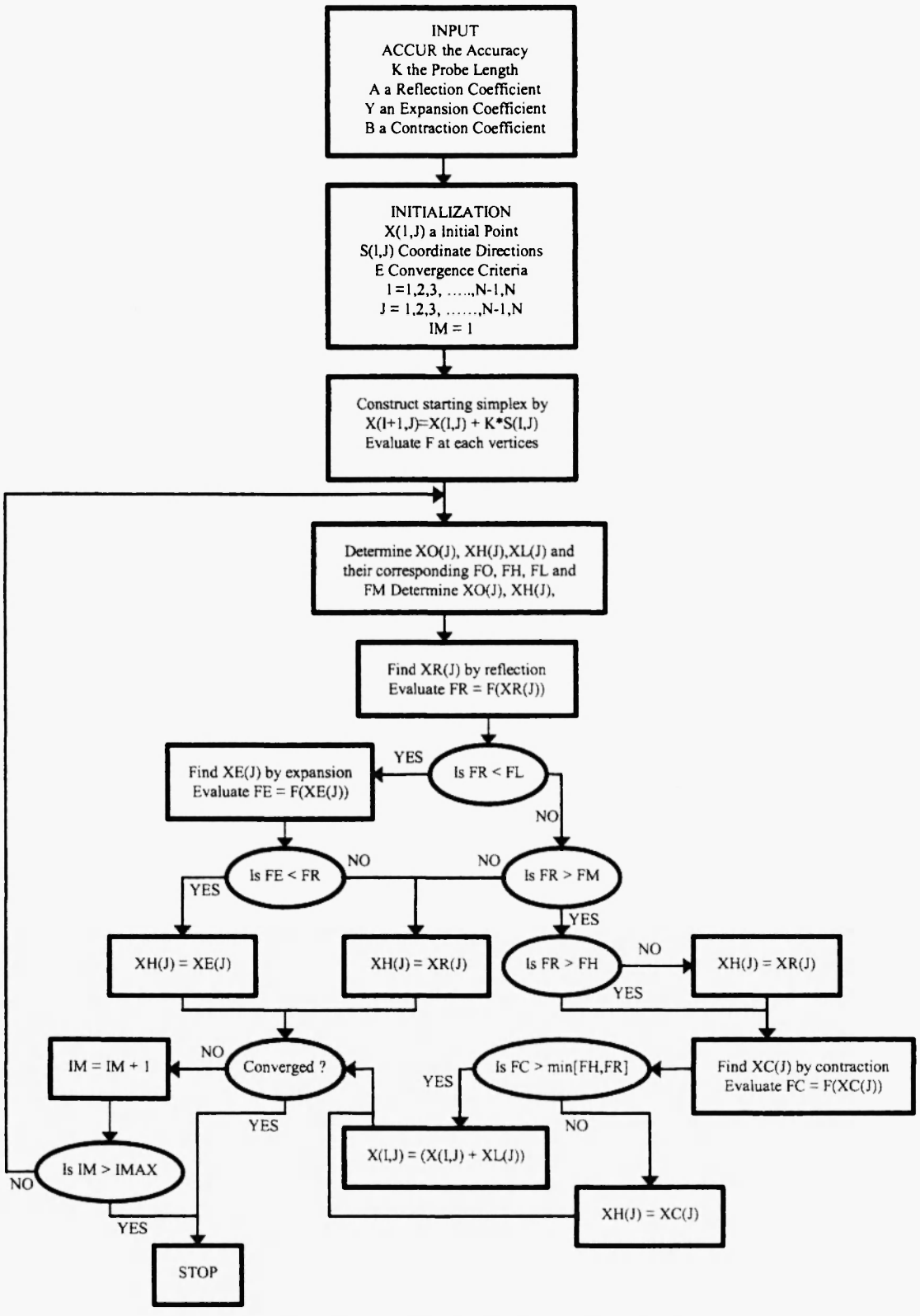

Fig. 15: Flowchart of "Simplex Optimization Method".

Table 2

Optimization results for various starting points Y^T.

Starting Point	Fibre Off-Axis Angle θ (°)	Fibre Aspect Ratio l/d	Fibre Volume Fraction V_f (%)	Local Minima
[0, 0, 0]	44.4	1.49	60.6	0.5833
[0.5, 0.5, 0.5]	43.9	83.6	54.2	0.5827
[1.0, 1.0, 1.0]	43.9	66.7	54.6	0.5828
[2.5, 2.5, 2.5]	44.1	1.46	60.8	0.5832
[5.0, 5.0, 5.0]	43.9	97.4	54.3	0.5827
[7.5, 7.5, 7.5]	44.3	38.2	55.2	0.5830
[10, 10, 10]	43.7	49.7	54.3	0.5829
[15, 15, 15]	44.0	1.47	60.8	0.5832
[20, 20, 20]	43.7	100.0	54.1	0.5827
[25, 25, 25]	43.0	1.05	65.0	0.5837
[30, 30, 30]	43.7	99.8	54.2	0.5827
[35, 35, 35]	43.5	97.0	54.0	0.5827
[40, 40, 40]	44.2	1.44	60.6	0.5832
[45, 45, 45]	43.8	99.1	54.0	0.5827
[50, 50, 50]	43.7	57.9	54.8	0.5828
[55, 55, 55]	43.7	72.6	53.8	0.5828
[60, 60, 60]	43.3	97.2	53.6	0.5827
[65, 65, 65]	43.4	95.3	53.8	0.5827
[70, 70, 70]	43.7	96.4	54.2	0.5827
[75, 75, 75]	43.4	99.1	53.9	0.5827
[80, 80, 80]	44.8	88.0	54.2	0.5827
[85, 85, 85]	43.8	75.1	54.1	0.5827
[90, 90, 90]	43.5	84.8	54.1	0.5827
[95, 95, 95]	43.2	89.4	53.7	0.5827

Thus, it could be concluded from the above results that, at the small fiber off-axis angle $\theta \approx 43.75^{\circ}$ and by approximately setting fiber aspect ratio at $l/d \approx 1.38$ or $l/d \approx 85$, the corresponding fiber volume fraction V_f reaches about 62% or 54% respectively, we could get maximum damping η_x, relatively high stiffness E'_x and relatively low specific weight $\bar{W}$.

4. CONCLUSIONS

The following conclusions may be drawn of the results obtained in this research:

(i) Analytical predictions which were determined by the "*Force-Balance Method*" show that damping and stiffness are functions of fiber off-axis angle, fiber volume fraction and fiber-aspect-ratio. In order to increase the damping, it is necessary to sacrifice the stiffness, and vice versa.

(ii) For a given E-glass/epoxy composite material, the results of optimizing the damping, stiffness and specific weight show that, approximately at a fiber off-axis angle $\theta \approx 43.75^{o}$, by setting the fiber-aspect-ratio $l/d \approx 1.38$ or $l/d \approx 85$, the corresponding fiber volume fraction V_f reaches 62% or 54%, one could obtain maximum damping, relatively high stiffness and relatively low specific weight for this class of material.

(iii) The existence of multiple local minima gives more flexibility in the design of high performance short-fiber reinforced composites, that is, in this research, both the microfiber or whisker composites ($l/d \approx 1.38$) and the short-fiber reinforced composites with longer fiber ($l/d \approx 85$) can be selected as to the predefined design specifications.

(iv) The "*Inverted Utility Function Method*" and "*Simplex Method*" were found to be suitable to deal with the multiobjective optimisation problem with a relatively small number of variables. The use of the "*Variable Transformation Technique*" to convert the constrained non-linear optimisation problem into a non-constrained non-linear optimisation makes such an optimisation problem much easier to handle.

ACKNOWLEDGMENTS

This research was supported by an operating research grant, to the first author, from Natural Sciences and Engineering Research Council of Canada.

5. REFERENCES

1. A.D. Nashif, D.I.G. Jones and J.P. Henderson. *Vibration Damping*, Wiley, New York, 1965.
2. R.F. Gibson and A. Yau. "Complex moduli of chopped fiber and continuous fiber composites: Comparison of measurements with estimated bounds", *Journal of Composite Materials,* **14**, 155-67 (1980).
3. R.F. Gibson, S.K. Chaturvedi and C.T. Sun. "Complex moduli of aligned discontinuous fiber-reinforced polymer composites", *Journal of Materials Science,* **17**, 1982, 3499-509 (1982).
4. C.T. Sun, R.F. Gibson and S.K. Chaturvedi. "Internal materials damping of polymer matrix composites under off-axis loading", *J. Material Science* **20**, 2575-85 (1985).

5. S.A. Suarez, R.F. Gibson, C.T. Sun and S.K. Chaturvedi. "The influence of fiber length and fiber orientation on damping and stiffness of polymer composite materials", *Experimental Mechanics,* **6**, 175-84 (1986).
6. C.M. Bert and R.R. Clary. *Composite Materials: Testing and Design*, ASTM STP 546-The American Society for Testing and Materials, Philadelphia, 1974; pp.250-65.
7. C.M. Bert. "Damping applications for vibrations controls", ASME AMD-38, *The American Society of Mechanical Engineers*, New York, 1980; pp.53-63.
8. D. Melean and B.E. Read. "Storage and loss moduli in discontinuous composites", *Journal of Materials Science,* **10**, 481-92 (1975).
9. H.L. Cox. "The elasticity and strength of paper and other fibrous materials", *British Journal of Applied Physics,* **3**, 72-84 (1952).
10. Z. Hashin. "Complex moduli of viscoelastic composites. I. General theory and application to particulate composites", *International Journal Solids and Structure*, **6**, 539-52 (1970).
11. Y.M. Haddad. *Viscoelasticity of Engineering Materials*, Kluwer, Dordrecht, 1995.
12. Y.M. Haddad (Editor). *Advanced Multilayered and Fiber-Reinforced Composites*, Kluwer, Dordrecht, 1998.
13. Y.M. Haddad. *Mechanical Behaviour of Engineering Materials,* Volumes I & II, Kluwer, Dordrecht, 2000.
14. B.D. Agarwal and L.J. Broutman. *Analysis and Performance of Fiber Composites*, Wiley Interscience, New York, 1980
15. J. Feng. *On the Viscoelastic Response of Laminated Composites*, Masters Thesis, University of Ottawa, Ottawa, Canada, 1999.
16. R.F. Gibson and R. Plunkett. "Dynamic mechanical behaviour of fiber reinforced composites: Measurement and analysis", *Journal of Composite Materials,* **10**, 325-41 (1976).
17. S.S. Rao. *Optimization: Theory and Applications*, Wiley Eastern Limited, Second Edition, 1984; pp.649-51.